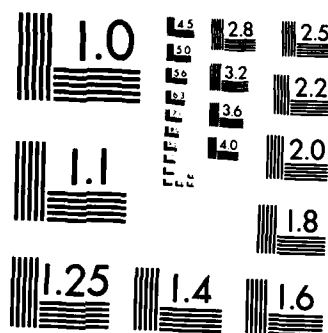


ON SIZE EFFECTS IN PLANE STRESS CRACK-GROWTH RESISTANCE  
(U) HARVARD UNIV CAMBRIDGE MA DIV OF APPLIED SCIENCES  
B BUDIANSKY ET AL. APR 85 MECH-68 N00014-84-K-0510

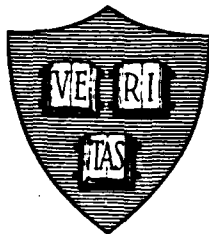
NL

F/G 20/11

Fi, NiO



AD-A155 926



(12)  
E/M

MECH-68

ON SIZE EFFECTS IN PLANE STRESS CRACK-GROWTH RESISTANCE

Bernard Budiansky and Eric E. Sumner, Jr.

DTIC  
ELECTE  
JUN 26 1985  
S B

**DISTRIBUTION STATEMENT A**

Approved for public release  
Distribution Unlimited

Division of Applied Sciences  
HARVARD UNIVERSITY  
Cambridge, Massachusetts 02138

April 1985

*To be presented at the 19th Midwestern Mechanics Conference,  
Ohio State University, Columbus, Ohio, September 9-11, 1985.  
To be published in "Developments in Mechanics", Volume 13.*

DTIC FILE COPY

## ON SIZE EFFECTS IN PLANE STRESS CRACK-GROWTH RESISTANCE

Bernard Budiansky  
Division of Applied Sciences, Harvard University  
Cambridge, Massachusetts 02138

Eric E. Sumner, Jr.  
AT&T Bell Laboratories  
Murray Hill, New Jersey 07974

## Abstract

For a ductile material, the tearing resistance curve represented by the dependence of the fracture parameter  $J$  on crack extension  $\Delta a$  is a material property only for the small-scale yielding conditions that are approached for very large specimen size. In this paper the influence of size on crack-growth resistance is studied theoretically for single-edge-notch (SEN) specimens of ideally-plastic materials in plane stress. The calculations are based on the Dugdale model in conjunction with a crack-growth criterion defined by an invariant crack-opening shape. Over a large range of specimen sizes, results are exhibited for materials having low-to-moderate values of initial tearing resistance.

Introduction

The initiation of mode I crack growth in ductile materials is governed, under broad circumstances, by a critical value of the Rice J-integral. Subsequent to initiation, increasing values of  $J$  may accompany crack growth, and the consequent relation between  $J$  and the growth  $\Delta a$  is called the tearing resistance curve. Although often tacitly regarded in the past as a material property, the function  $J(\Delta a)$  is size and configuration dependent. At the very least, the size of a specimen sets an upper bound on the maximum possible value of crack size that can be attained in a test.

In this paper, we consider plane stress, and use the Dugdale model to study crack growth in an elastic-ideally plastic material. We adopt a crack-growth criterion that rests on the assumption of an invariant, crack-opening shape near the crack tip during crack extension. (This criterion is mathematically equivalent to the "first-stretch" criterion proposed by Wnuk (1972), and has been used by Rice et al. (1980) for plane strain crack growth.) We will first discuss the resistance curve for small-scale yielding, which is considered to be a material property, and applies to the limiting

case of infinite specimen size. Attention will then be focused on the single-edge-notch (SEN) configuration, for which calculations have been made on the basis of an approximate numerical analysis (the details of which will be reported elsewhere). Theoretical nondimensional resistance curves will be shown for a wide range of specimen size, and compared with the small-scale yielding curve. Finally, a recent proposal by Hellmann and Schwalbe (1984) for correlating resistance curves on the basis of a special crack-opening displacement will be discussed briefly.

#### Dugdale Model; Crack-Growth Criterion

Figure 1(a) shows crack-tip parameters associated with the Dugdale model of a stationary crack of length  $a_0$ . The shaded region shows the plastic stretch ahead of the crack tip in a zone where the yield stress  $\sigma_y$  is attained. The crack opening displacement  $\delta(r)$  near the crack tip is

$$\delta(r) \sim \delta_{\text{tip}} + \left( \frac{4\epsilon_y}{\pi} \right) r \log[c(J,a)/r] \quad (1)$$

where (Rice, 1968),  $\delta_{\text{tip}} = J/\sigma_y$ ,  $\epsilon_y = \sigma_y/E$ , and the length  $c$  depends on the specimen size and configuration as well as  $J$  and  $a$ . The crack starts growing at  $J = J_c$ , when  $\delta_{\text{tip}} = \delta_c = J_c/\sigma_y$ . Near the advancing crack tip (Fig. 1(b)) the opening displacement is

$$\begin{aligned} \Delta(r) &\sim \frac{J(a)}{\sigma_y} + \left( \frac{4\epsilon_y}{\pi} \right) r \log[c(J,a)/r] - \frac{J(a-r)}{\sigma_y} \\ &\sim \left( \frac{4\epsilon_y}{\pi} \right) r \log \left[ \frac{c(J,a) \exp \left( \frac{\pi}{4\sigma_y \epsilon_y} \frac{dJ}{da} \right)}{r} \right] \end{aligned} \quad (2)$$

A first-order differential equation governing the relationship  $J(a)$  follows from the assumption that  $\Delta(r)$  remains invariant during crack growth. This gives

$$\frac{E}{\sigma_y^2} \frac{dJ}{da} = \frac{4}{\pi} \log \left[ \frac{A}{c(J,a)} \right] \quad (3)$$

where the characteristic length  $A$  is a material constant. The initial condition that goes with (3) is  $J(a_0) = J_c$ , and the length  $A$  will be related to the tearing modulus (Paris et al., 1979)

$$T_s = \frac{E}{\sigma_y^2} \left( \frac{dJ}{da} \right)_s \quad (4)$$

that corresponds to the initial slope  $\left( \frac{dJ}{da} \right)_s$  of the resistance curve of small-scale yielding.

#### Small-Scale Yielding

In small-scale yielding,

$$c = \frac{\pi}{2} \frac{EJ}{\sigma_y^2} \quad (5)$$

and so it follows from (3) that

$$A = \frac{\pi EJ}{2\sigma_y^2} \exp(\pi T_s/4)$$

Henceforth, we regard  $T_s$  as the more useful material parameter, in lieu of  $A$ . A general crack-growth differential equation, for arbitrary configurations, now follows from Eq. (3) as

$$\frac{d(J/J_c)}{d\eta} = T_s - \frac{4}{\pi} \log \left[ \left( \frac{2\epsilon_y}{\pi \delta_c} \right) c(J,a) \right] \quad (6)$$

where

$$\eta = (\Delta a) \epsilon_y / \delta_c \quad (7)$$

is a convenient nondimensional crack-extension variable.

The resistance curve for small-scale yielding is given by the solution of

$$\frac{d(J/J_c)}{d\eta} = T_s - \frac{4}{\pi} \log(J/J_c) \quad (8)$$

which follows from the substitution of (5) into (6). With  $J/J_c = 1$  at  $\eta = 0$ , this produces

$$\eta = \frac{\pi}{4} e^{\pi T_s/4} \{E_1[\pi T_s/4 - \log(J/J_c)] - E_1[\pi T_s/4]\} \quad (9)$$

where  $E_1(x) = \int_x^\infty (e^{-\rho}/\rho) d\rho$ . (An analogous small-scale yielding solution is shown by Rice and Sorensen (1978) for plane-strain.)

Nondimensional resistance curves for small-scale yielding are illustrated in Fig. 2 for  $T_s = 2, 5, 10$ . For  $\eta \rightarrow \infty$ ,  $J/J_c$  approaches the asymptotic, steady-state value  $\exp[\pi T_s/4]$ . Note that even for low values of  $\delta_c/\epsilon_y$  ( $\sim 1$  cm) practical limitations on specimen size would permit a close approach to steady-state cracking only for low values of  $T_s$ .

#### SEN Specimens: Effect of Size on Initial Tearing Modulus

By means of an approximate method (details of which will be published elsewhere) a method has been devised for estimating  $c(J,a)$  in Eq. (1) for the single-edge-notch (SEN) specimen shown in Fig. 3. If we introduce the specimen-size parameter

$$\Lambda = W \epsilon_y / \delta_c \quad (10)$$

the second term in Eq. (6) is found to depend only on  $J/J_c$ ,  $\Lambda$ , and the crack-width ratio  $a/W$ . The initial tearing modulus of the SEN specimen

$$T_0 = \frac{E}{\sigma_y^2} \left( \frac{dJ}{da} \right)_0 \quad (11)$$

is then given by (6) for  $a=a_0$ , the initial crack size, and  $J/J_c=1$ . The resulting difference  $(T_0-T_s)$  is shown in Fig. 4 as a function of  $a_0/W$ , for specimen sizes between  $\Lambda=2$  and  $\Lambda=50$ . Of particular note are the facts that (i)  $(T_0-T_s)$  does not depend on  $T_s$ ; (ii)  $|T_0-T_s|$  decreases rapidly with increasing  $\Lambda$ ; (iii) as a function of  $a_0/W$ ,  $(T_0-T_s)$  changes sign in the vicinity of  $a_0/W \approx .25$ ; (iv) for all reasonable  $a_0/W$ , and for all sizes  $\Lambda$ , the relative error  $(T_0-T_s)/T_s$  would be negligible for moderate to large values of  $T_s$ , and is negligible for all  $T_s$  for  $a_0/W$  near  $1/4$ . Thus, the choice  $a_0 \approx W/4$  should eliminate any concern about the effect of specimen size on initial tearing modulus.

#### SEN Specimens; Effect of Size on Resistance Curves

Introduction of the aforementioned estimate for  $c(J,a)$  into the differential equation (6) and its subsequent integration permits the derivation of nondimensional resistance curves of  $J/J_c$  vs.  $\eta$ , for various values of  $a_0/W$ ,  $\Lambda$ , and  $T_s$ . For  $a_0/W = .25$ , we show results in Figs. 5-7 for  $T_s = 2, 5$ , and  $10$ . In each case, the small-scale yielding (SSY) curve, which applies for  $\Lambda \rightarrow \infty$ , is shown together with resistance curves for  $\Lambda = 2, 5, 10, 20$ , and  $50$ . The curves for finite  $\Lambda$  terminate well before the values  $\eta = \Lambda(1-a_0/W)$  that correspond to cracking across the full specimen width because the underlying approximations become inaccurate. In particular, yielding in compression at the back face has been ignored. In all cases, however, the applied load corresponding to the ends of the curves is below the fully-plastic limit load of the cracked specimen, and is usually well below this limit when the curves begin to deviate from the SSY result.

For each  $T_s$  and  $\Lambda$  the resistance curve peels off from the SSY result after a certain amount of crack growth that decreases markedly with decreasing  $\Lambda$ . Following Hellmann and Schwalbe (1984), we will let  $(\Delta a)_{05}$  correspond to a 5% reduction of  $J/J_c$  from its SSY value. For each  $T_s$ ,  $\eta_{05} = (\Delta a)_{05} E_y / \sigma_c$  appears roughly proportional to  $\Lambda$ . Indeed, as shown in Fig. 8, the quantity  $(\Delta a)_{05} / (W-a_0)$ , representing fractional penetration into the uncracked ligament, is a weak function of  $\Lambda$ , but decreases with increasing  $T_s$ . Note that for  $a_0/W = 1/4$ ,  $T_s \leq 10$ , and  $\Lambda > 5$ , the crack can grow into at least 20% of the initially uncracked ligament without serious deviation from the SSY resistance curve.

Calculations of resistance curves for other values of  $a_0/W$  give results similar to those of Figs. 5-7. For the case  $a_0/W = 1/2$ , the values

found for  $(\Delta a)_{05}/(W-a_0)$  are shown in Fig. 9. Here the allowable penetration is smaller than for  $a_0/W=1/4$ , but varies less with  $T_s$ .

Corresponding to each of the resistance curves shown in Figs. 5-7, the variations of  $\sigma/\sigma_y$  with  $a/W=(a_0+\Delta a)/W$  are plotted in Figs. 10-12. The dependence on  $a/W$  of the fully-plastic limit-load value of  $\sigma/\sigma_y$  is also shown. The lines across the curves connect the points  $(a/W)_{05}=[a_0+(\Delta a)_{05}]/W$ , for which  $J/J_c$  deviates by 5% from SSY. Note that the stress always peaks before this crack length is reached. It is evident that the present calculations of  $(a/W)_{05}$  will become unreliable for higher values of  $T_s$ , because the stress will get too close to the fully-plastic limit load. Nevertheless, it appears that the trend established for  $(a/W)_{05}$  will continue for  $T_s > 10$ , with significant deviation from the SSY resistance curve occurring at still smaller crack extensions.

#### Hellmann-Schwalbe COD vs. Crack Growth

Hellmann and Schwalbe (1984) have suggested that the crack-opening-displacement (COD) just behind the original crack tip might correlate well with crack-growth, and be less size-dependent than  $J$  vs.  $\Delta a$ . We denote this COD by  $\delta^*$ , and show in Figs. 13-15 calculated curves of  $\delta^*/\delta_c$  vs.  $\eta$  for the cases studied in Figs. 5-7. It can be seen that the correlation is indeed a little better, but that the curves all eventually become concave upward. Indeed, it might be suggested that curvature reversal in the  $\delta^*$  vs.  $\Delta a$  relation is a clear signal that the SSY resistance curve is no longer applicable. Note, too, that the  $\delta^*$  curves tend to undershoot the SSY result slightly before they turn upward.

#### Concluding Remarks

The most comforting conclusion to be drawn is that over a very large range of SEN specimen sizes, the choice  $a_0/W \approx 1/4$  eliminates size effects on the initial tearing modulus. Resistance curves do display strong size effects, but for given values of  $a_0/W$  and  $T_s < 10$ , sharp deviations from the small-scale yielding curve begin at relative crack penetrations  $(\Delta a)/(W-a_0)$  that do not vary much with size. These conclusions will not, of course, necessarily hold for configurations other than SEN, nor necessarily for strain-hardening materials. The Hellmann-Schwalbe COD is a little better than  $J$  as a correlating function for crack growth. Another correlation parameter, the Ernst (1983)  $J_M$  should be mentioned, but its theoretical performance on the basis of the present theory has not been studied.

#### Acknowledgements

This work was supported in part by the Office of Naval Research under Contract N00014-84-K-0510, by the National Science Foundation under Grant MEA-82-13925, and by the Division of Applied Sciences, Harvard University.

✓  
PER  
LETTER



Dist

A-1



### References

- Ernst, H. A., (1983), Proc. 14th Nat. Symp. Fract. Mech., ASTM STP 791, Vol. I, 499-519.
- Hellmann, D. and Schwalbe, R. H., (1984), Proc. 15th Nat. Symp. Fract. Mech., ASTM STP 833.
- Paris, P. C., Tada, H., Zahoor, A. and Ernst, H. A., (1979), ASTM STP 668, 5-36.
- Rice, J. R., (1968), in Fracture, Academic Press, ed. H. Liebowitz, Vol. II, 264.
- Rice, J. R. and Sorensen, E. P., (1978), J. Mech. Phys. Solids, 26, 163-186.
- Rice, J. R., Drugan, W. J. and Sham, T. L., (1980), ASTM STP 700, 189-219.
- Wnuk, M. P., (1972), Proc. Int'l. Conf. Dynamic Crack Propagation, Lehigh University, 273-280.

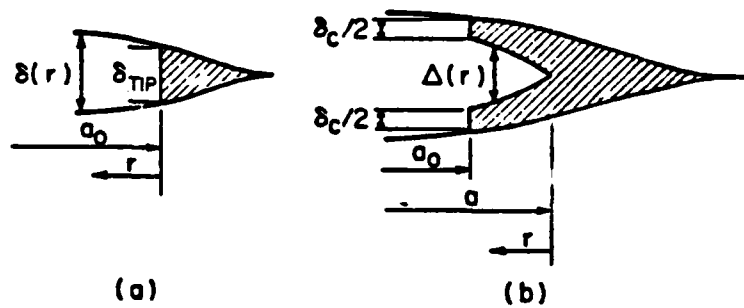


Fig. 1 Crack-tip parameters, Dugdale model  
(a) stationary crack, (b) growing crack.

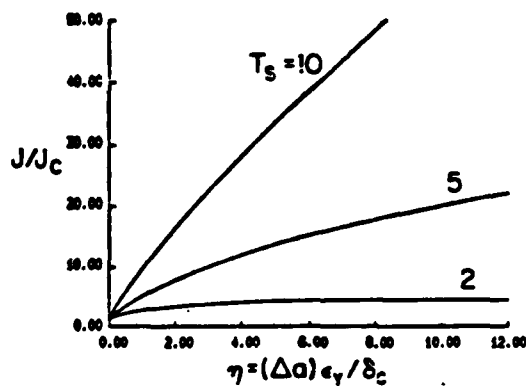


Fig. 2 Small-scale yielding resistance curves.

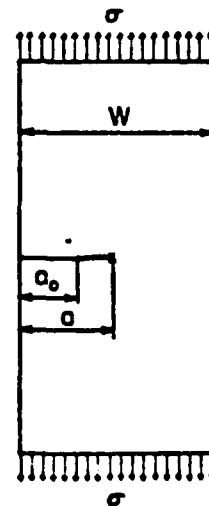


Fig. 3 SEN specimen.

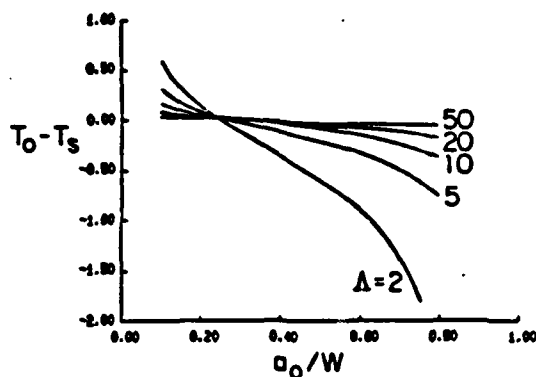


Fig. 4 Size effect on initial tearing modulus  $T_s$ .

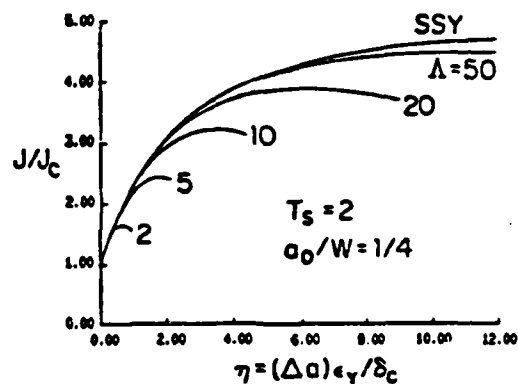


Fig. 5 Resistance curves,  $T_s = 2$ .

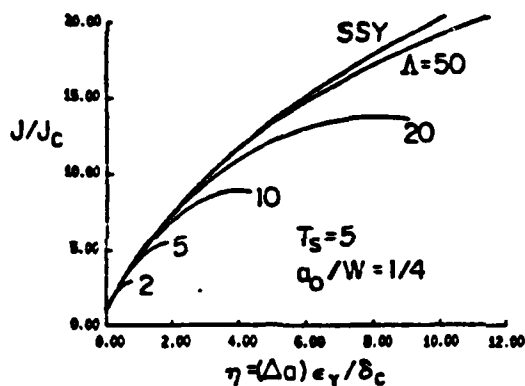


Fig. 6 Resistance curves,  $T_s = 5$ .

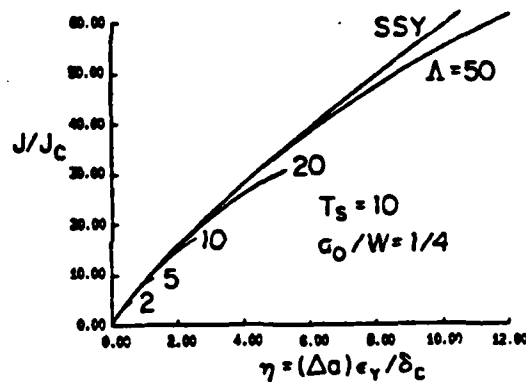


Fig. 7 Resistance curves,  $T_s = 10$ .

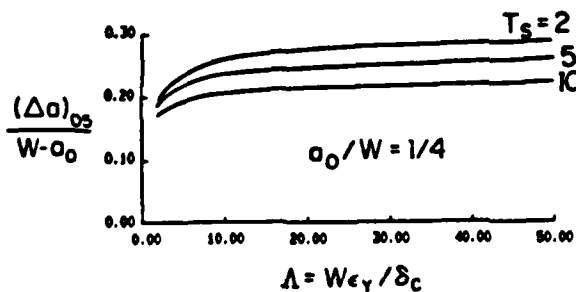


Fig. 8 Allowable crack penetration,  $a_0/W = 1/4$ .

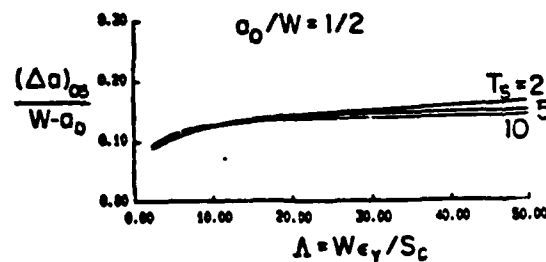


Fig. 9 Allowable crack penetration,  $a_0/W = 1/2$ .

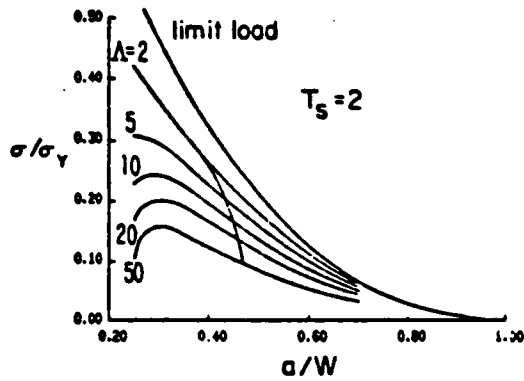


Fig. 10 Stress history,  $T_s = 2$ .

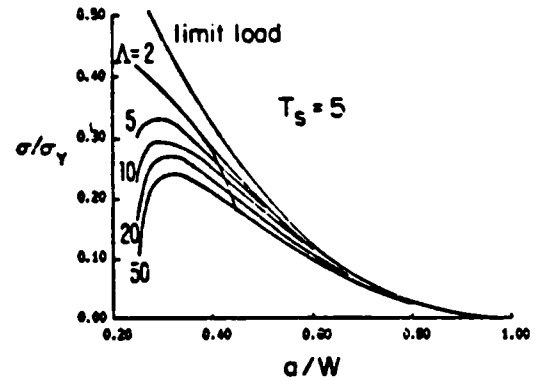


Fig. 11 Stress history,  $T_s = 5$ .

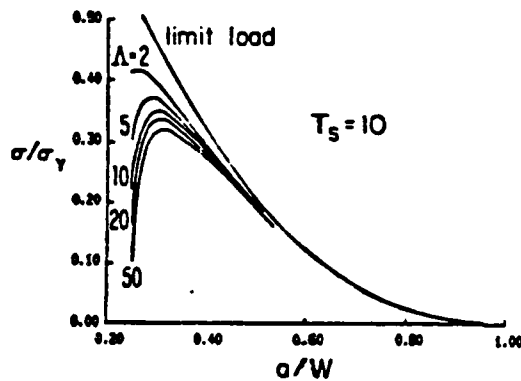


Fig. 12 Stress history,  $T_s = 10$ .

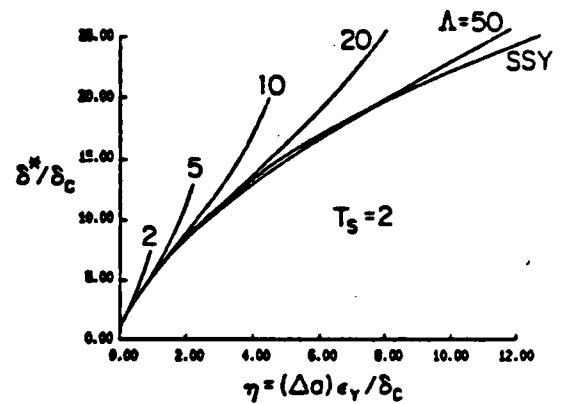


Fig. 13 COD curves,  $T_s = 2$ .

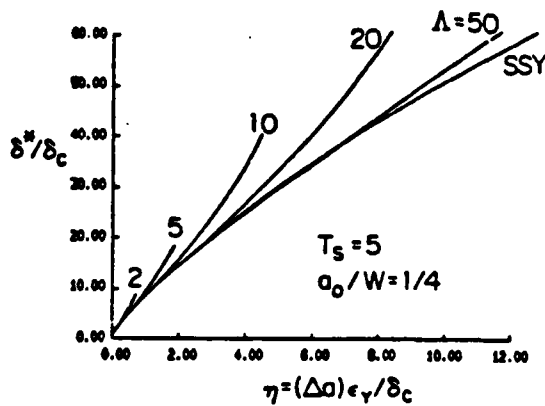


Fig. 14 COD curves,  $T_s = 5$ .

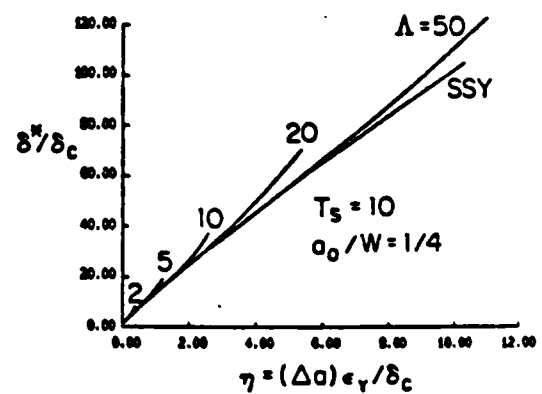


Fig. 15 COD curves,  $T_s = 10$ .

**END**

**FILMED**

**8-85**

**DTIC**